Title
POLARIZATION OF NUCLEONS SCATTERED ELASTICALLY BY NUCLEI

Authors
Fernbach, Sidney
Heckrotte, Warren
Lepore, Joseph V.

Publication Date
1954-10-13

UNIVERSITY OF CALIFORNIA

Radiation Laboratory

BERKELEY, CALIFORNIA

DISCLAIMER

UCRL-2749
Unclassified Physics

or
Phys. Rev. 97, 1059 (195
Feb. 15

UNIVERSITY OF CALIFORNIA

Radiation Laboratory

Berkeley, California

Contract No. 7405-eng-48

POLARIZATION OF NUCLEONS SCATTERED ELASTICALLY BY NUCLEI

Sidney Fernbach, Warren Heckrotte and Joseph V. Lepore

Printed for the U.S. Atomic Energy Commission

UCRL-2749

POLARIZATION OF NUCLEONS SCATTERED ELASTICALLY BY NUCLEI

Sidney Fernbach, Warren Heckrotte and Joseph V. Lepore

Radiation Laboratory, Department of Physics
University of California, Berkeley, California

October 13, 1954

ABSTRACT

A study of the nucleon polarization to be expected when nucleons are elastically scattered from nuclei is presented. The polarization effect is a consequence of the fact that the nucleon-nucleus interaction may be represented as a complex spin-dependent potential. The existence of such an potential is suggested by the nuclear shell model and the spin dependence of the nucleon-nucleon interaction. Qualitative arguments are advanced to determine this potential in terms of the nucleon-nucleon interaction. Although the polarization effect is by no means confined to elastic scattering it is in this case particularly useful since the large diffraction cross sections observed experimentally insure relatively high yields of polarized particles. A number of studies have been carried out, for both neutron and proton scattering, which show that almost full polarization can occur. The calculations have been carried out using the W.K.B. approximation as usually applied to the nuclear optical model. The method has been checked by carrying out an exact phase shift analysis for a particular case. The results show that studies of nucleon polarization can illuminate some aspects of nuclear structure since the polarization depends on the particular nucleus used as a target as well as upon the form of the interaction.

POLARIZATION OF NUCLEONS SCATTERED ELASTICALLY BY NUCLEI

Sidney Fernbach, Warren Heckrotte and Joseph V. Lepore

Radiation Laboratory, Department of Physics
University of California, Berkeley, California

I. INTRODUCTION

The existence of a nucleon-nucleus spin dependent interaction is suggested by the fact that the nucleon-nucleon potential is itself spin dependent[1]; moreover such an interaction is an essential feature of the nuclear shell model.

Such an interaction should manifest itself in a polarization of nucleons scattered by nuclei.[2] Although the polarization effect is by no means confined to the case of elastic scattering this process is particularly interesting and useful since the large diffraction cross sections found experimentally insure a relatively high yield of polarized particles.

The elastic scattering of nucleons by nuclei can be described by the treating the nucleon-nucleus interaction as a complex potential.[3] The imaginary part of the complex potential represents the effect of all processes not leading to elastic scattering. If in addition to a complex central potential there exists a spin dependent potential the elastic scattered nucleons will be polarized. As a consequence of the complex potential a Born approximation treatment of the scattering will lead to a non-vanishing polarization in distinction to the case of a purely real potential where the Born approximation always leads to no polarization since it leaves intact the relative phase relations of waves of different values of the orbital angular momentum.

For low energy nucleon scattering one may expect that the polarization will reflect the characteristics of the spin-orbit potential of the shell model but at high energies it is certainly more sensible to expect that the nucleon-nucleon potential is directly effective[4] since the incident particle can then "see" individual nucleons in the nucleus.

An estimate of the polarization effect for a spin zero nucleus can be made by assuming a complex spin dependent interaction of the form

$$V(\vec{r}) = V_c(\vec{r}) + V_s(\vec{r})\vec{\sigma}\cdot\vec{L} \quad . \tag{1}$$

Here $\vec{\sigma}$ and $\vec{L}$ represent the spin and orbital angular momentum of the nucleon; V_c and V_s are in general complex potentials depending on the nucleon coordinate $\vec{r}$. The parameters characterizing them should be chosen to fit as well as possible the observed data on nucleon-nucleus scattering. The scattering cross section and polarization to be expected from such a potential are given by[5]

$$\frac{d\sigma}{d\Omega} = A + B\vec{\sigma}\cdot\vec{n} \tag{2}$$

and

$$\vec{P}(\theta) = \frac{AB^* + A^*B}{d\sigma/d\Omega}\,\vec{n} \quad . \tag{3}$$

A and B represent the amplitudes for spin independent and spin dependent scattering respectively. The vector $\vec{n}$ is the normal to the plane of scattering and is determined by

$$\vec{k} \times \vec{k}' = \vec{n}\,k^2 \sin\theta \, , \tag{4}$$

where $\vec{k}$ and $\vec{k}'$ are the initial and final momenta, respectively.

To make a crude estimate of $\vec{P}$ valid at small angles for the case of carbon, V_s will be assumed to be real square well of size $1.4\,A^{1/3} \times 10^{-13}$ cm and of 2 Mev in depth. If B is estimated by the Born approximation it is purely imaginary. As a consequence one need only know the imaginary part of A. For small angles this is approximately proportional to the total cross section for nucleon-nucleus scattering.

$$\text{Im } A \cong \frac{k\sigma_T}{4\pi} \quad . \tag{5}$$

One may therefore use the known experimental values[6] for σ_T and $d\sigma/d\Omega$ in this formula and in the denominator of Eq. (3). These values $\sigma_T = 0.288 \times 10^{-24}$ cm^2, and $\frac{d\sigma}{d\Omega}(5^\circ) = 0.725 \times 10^{-24}$ cm^2 yield a polarization at $\theta = 5^\circ$,

$$\left| P(5^\circ) \right| \sim 40\% \tag{6}$$

for 300 Mev neutrons incident on carbon.

II. THE NUCLEON-NUCLEUS INTERACTIONS

The nucleon-nucleus interaction for a spin zero nucleus, must be linear in the spin vector $\vec{\sigma}$. Accordingly, the usual optical model of the nucleus can be generalized by the addition of a spin-orbit potential[7]:

$$V = V_c + V_s \vec{\sigma} \cdot \vec{L} \ . \tag{7}$$

V_c, the central potential, is in general complex, and is usually taken to be of some simple algebraic form which is assumed to be proportional to the density of nucleons in the nucleus. The functional form of V_s can be conjectured[8] (by the analogy with spin-orbit potentials in a number of other instances) to be of the form,

$$V_s(r) \sim \frac{1}{r} \frac{d}{dr} V_c(r) \ , \tag{8}$$

(although in general V_s is a complicated integral operator). Rather than appeal to these analogous situations, however, one can show that a similar dependence is a simple consequence of the nucleon-nucleon interaction.

We begin with the identity

$$V\psi_o = \frac{1}{(2\pi)^3} \int e^{i\vec{k}\cdot\vec{x}} \, d\vec{x} \int e^{-i\vec{k}\cdot\vec{r}} \, V \psi_o \, d\vec{r} \ , \tag{9}$$

where V is the optical model potential and ψ_o is the wave function describing the elastic scattering of the incident nucleon. V, in general, can be a differential or integral operator. We assume now that the equivalent potential of the nucleon-nucleus interaction which describes elastic scattering --the optical model potential--can be expressed in terms of the individual

nucleon-nucleon scattering process. That is, we write

$$V\psi_o(x) = \frac{1}{(2\pi)^3}\int e^{i\vec{k}_f\cdot x}\, d\vec{k}_f \int e^{-i\vec{k}_f\cdot\vec{r}_o}\, \phi_o^*(1,\ldots,n)\sum_\kappa T_\kappa\, \phi_o(1,\ldots,n)\, \psi(r_o)\, d\vec{r}_o\, d\vec{r}_1 \ldots d\vec{r}_n \,. \tag{10}$$

$\phi_o(1,\ldots,n)$ is the ground state nuclear wave function. T_κ is the transition matrix for scattering between the incident and the κ'th nucleon. In a momentum representation, T_κ has the form[9]

$$(\vec{k}'\,|\,T_\kappa\,|\,\vec{k}) = a(\vec{k}',\vec{k}) + i\vec{\sigma}_o(\vec{k}' \times \vec{k})\, b(\vec{k}',\vec{k}) + (\text{terms containing } \vec{\sigma}_\kappa)\,. \tag{11}$$

We will limit ourselves to spin zero nuclei so that terms of T_κ containing σ_κ will drop out.

The equivalent potential as defined by Eq. (10) is subject to several assumptions. These are the impulse approximation[10] and a partial neglect of multiple scattering.[11] Subsequent assumptions which are necessary to reduce this expression to a more tractable form, amount to a complete neglect of the role of multiple scattering in defining the potential.

To evaluate Eq. (10) we will assume that the nuclear wave function can be represented by the independent particle model,

$$\phi_o(1,\ldots,n) = \frac{1}{\sqrt{n}}\sum_P (-)^P \phi_{q_1}(r_1)\ldots\phi_{q_n}(r_n) \,. \tag{12}$$

This specialization is not necessary but it simplifies the formal manipulations. Introducing the Fourier transforms $\phi_{q_K}(\vec{k})$ and $\psi_o(\vec{k})$ of $\phi_{q_K}(\vec{r})$ and $\psi_o(\vec{r})$ respectively, Eq. (10) becomes

$$V\psi_o = \frac{1}{(2\pi)^{9/2}} \int e^{-i\vec{k}_f\cdot\vec{x}}\, d\vec{k}_f \left\{ \sum_{q_K} \phi^*_{q_K}(\vec{k}_o + \vec{k} - \vec{k}_f)\, \phi_{q_K}(\vec{k})\, \psi_o(\vec{k}_o) \right.$$

$$\left. \times \left(\frac{2\vec{k}_f - \vec{k}_o - \vec{k}}{2} \,\middle|\, T \,\middle|\, \frac{\vec{k}_o - \vec{k}}{2} \right) d\vec{k}_o\, d\vec{k} \right\} \tag{13}$$

Assuming that the functions a and b of Eq. (11) depend only on the momentum transfer for a given incident wave number[10], the T matrix in the above equation will be independent of $\vec{k}$. Or, one might assume, since it is presumed that $k_o >> k$, that it is safe to neglect the dependence of the T matrix on 1. In either case the above integral can be rewritten as

$$V\psi_o = \frac{1}{(2\pi)^3} \int e^{i\vec{k}_f\cdot\vec{x}}\, d\vec{k}_f\, e^{-i(\vec{k}_f - \vec{k}_o)\cdot\vec{r}}\, \rho(r) \left(\frac{2\vec{k}_f - \vec{k}_o}{2} \,\middle|\, T \,\middle|\, \frac{\vec{k}_o}{2} \right)$$

$$\times \psi_o(\vec{k}_o)\, d\vec{k}_o\, d\vec{r} \tag{14}$$

where

$$\rho(r) = \sum_{q_K} \left| \phi_{q_K}(\vec{r}) \right|^2 .$$

Substituting Eq. (11) for the T matrix and letting $\vec{g} = (\vec{k}_f - \vec{k}_o)$, one finds

$$V\psi_o = \frac{1}{(2\pi)^{3/2}} \int e^{i\vec{g}\cdot(\vec{x} - \vec{r})} \rho(r) \left[a(g, k_o) + i\vec{\sigma}_o \cdot (\vec{g} \times \vec{k}_o)\, b(g, k_o) \right] \times e^{i\vec{k}_o \cdot \vec{x}} \psi_o(k_o)\, d\vec{k}_o \quad . \tag{15}$$

The vectors $\vec{g}$ and $\vec{k}_o$ can be replaced by gradients operating on the appropriate exponential function. Assuming in addition that the functions $a(g, k_o)$ and $b(g, k_o)$ are independent of k_o over the range of values allowed by $\psi_o(k_o)$, one obtains,

$$V\psi_o = \left(V_1(\vec{x}) - i\vec{\sigma} \cdot \vec{\nabla} V_2(\vec{x}) \times \vec{\nabla} \right) \psi_o(\vec{x}) \tag{16}$$

where

$$V_1(\vec{x}) = \frac{1}{(2\pi)^{3/2}} \int e^{i\vec{g}\cdot(\vec{x} - \vec{r})} \rho(r)\, a(g)\, d\vec{g}\, d\vec{r} \quad ,$$

$$V_2(\vec{x}) = \frac{1}{(2\pi)^{3/2}} \int e^{i\vec{g}\cdot(\vec{x} - \vec{r})} \rho(r)\, b(g)\, d\vec{g}\, d\vec{r} \quad . \tag{17}$$

Since V_1 and V_2 are radial functions, we may write

$$V = V_1(x) + \frac{1}{x} \frac{d}{dx} V_2(x)\, \frac{\vec{\sigma} \cdot \vec{L}}{\hbar} \quad . \tag{18}$$

We note that $a(g)$ and $b(g)$ can be expressed as functions of angles in the nucleon-nucleon center of mass system by the relation $g = 2\bar{k} \sin \bar{\theta}/2$ where $\bar{k}$ and $\bar{\theta}$ are the wave number and angle of scattering

in the center of momentum system. In the nucleon-nucleus system, $g = 2k \sin \theta/2$ where k and θ are the wave number and angle of scattering in this system. The relation between the two is

$$k = 2\bar{k}$$

and (19)

$$\theta \sim \bar{\theta}/2.$$

Now if the extent of the density distribution is R, then the range of values over which a and b contribute is given from an examination of Eq. (17), by

$$g \sim \frac{\pi}{R} \tag{20}$$

or

$$\theta \sim \frac{\pi}{kR} \qquad (\text{or} \quad \bar{\theta} \sim \frac{2\pi}{kR}) .$$

Now, if a and b as a function of angle do not change appreciably over this angular range, the expressions for the potentials may be approximated by

$$V_1 = a(0)\, \rho(r)$$

(21)

$$V_2 = b(0)\, \rho(r) ,$$

where $a(0)$ and $b(0)$ are the values of a and b in the forward direction. These equations are just the familiar result expressing the equivalent potentials in terms of the forward scattering amplitude.[12]

It follows that the radial dependence of the spin orbit potential is indeed proportional to $\frac{1}{r}\frac{d}{dr} V_c(r)$. This does not however appear to be true in general, but only to the extent of the validity of the assumptions made in the derivation. At much lower energies (< 100 Mev) where one would expect multiple scattering to become quite important, this particular form of the spin orbit potential is questionable. It should be noted also that the coefficients of $\vec{\sigma}_K$ in the scattering matrix (Eq. (11)) would enter into the definition of the equivalent potential as a result of multiple scattering.

In most applications of the optical model, the coefficients $a(0)$ and $b(0)$ are, for a given radial dependence $\rho(r)$, fixed phenomenologically, so as to yield the diffraction and inelastic cross sections and the angular distribution. The scattering at large angles depends however on the specific angular behavior of a and b, and this is ignored in the usual applications of the optical model.

In the remainder of this paper the optical model potential will be written in the following form:

$$V = -(u + iw)\rho(r) + \frac{\mu a^2}{\hbar}\frac{1}{r}\frac{d}{dr}\rho(r)\vec{\sigma}\cdot\vec{L} \qquad (22)$$

where u, w, and μ are constants with the dimensions of energy and a is a constant of the dimension of length. The radial dependence of the central well is given by $\rho(r)$ which is normalized to unity for $r = 0$. The sign of the spin orbit potential is taken to be the same as for the spin orbit potential of the shell model, assuming that $\rho(r)$ is a radially decreasing function.

III. CALCULATIONS

The one particle Schroedinger equation for the scattering problem is

$$\left[-\frac{\hbar^2}{2m}\nabla_r^2 - (u+iw)\,\rho(r) + \frac{\mu a^2}{r}\frac{d}{dr}\rho(r)\,\frac{\vec{\sigma}\cdot\vec{L}}{\hbar}\right]\psi = \frac{\hbar^2 k^2}{2m}\psi\,, \tag{23}$$

where k is the incident wave number. The wave function ψ has the asymptotic form

$$\psi = e^{i\vec{k}\cdot\vec{r}}\chi_{inc} + f(\theta)\,\frac{e^{ikr}}{r} \tag{24}$$

where χ_{inc} is the spin function of the incident nucleon, and $f(\theta)$ is the amplitude of the scattered wave at infinity. From simple invariance arguments $f(\theta)$ must have in general the form

$$f(\theta) = \left[A(\theta) + \vec{\sigma}\cdot\vec{n}\,B(\theta)\right]\chi_{inc} \tag{25}$$

where $\vec{n}$ is the unit vector normal to the plane of scattering. For an unpolarized incident nucleon, the differential cross section and polarization are given by[5]

$$\frac{d\sigma}{d\Omega} = \left(|A|^2 + |B|^2\right) \times \left(\frac{2m}{\hbar^2}\right)^2$$

$$P = \frac{AB^* + A^*B}{|A|^2 + |B|^2}\,. \tag{26}$$

For the case of polarized incident nucleons, $\frac{d\sigma}{d\Omega}$ becomes,

$$\frac{d\sigma}{d\Omega} = \left(|A|^2 + |B|^2\right)\left[1 + P\,\vec{P}_{inc}\cdot\vec{n}\right] \qquad (27)$$

where $\vec{P}_{inc}$ is the polarization of the incident nucleons and $\vec{n}$ is defined as before.

In general one cannot hope to obtain an exact or explicit solution to this scattering problem. Accordingly, solutions will be obtained on the basis of two approximations. The first of these is the Born approximation and the second is the W.K.B. approximation applied to the evaluation of the phase shifts. As will be seen, one must go beyond the first Born approximation to bring out all of the features of the polarization phenomena.

A. Born Approximation

For high energies ($\sim$300 Mev) and for the lighter nuclei it has been pointed out[13] that the Born approximation yields a qualitative estimate of the amount and character of the polarization phenomena. The fact that the first Born approximation yield a polarization is a consequence of the use of a complex central potential.

The scattered amplitude can be readily evaluated in the Born approximation and is given by

$$\left(\frac{2m}{\hbar^2}\right)^{-1} f(\theta) = A(\theta) + \vec{\sigma}\cdot\vec{n}\, B(\theta)$$

where

$$A(\theta) = \int j_0(gr)(u + iw)\,\rho(r)\, r^2\, dr$$

$$B(\theta) = \frac{-i\,k^2 \sin\theta}{g} \int j_1(gr)\left(+\frac{\mu a^2}{r}\,\frac{d}{dr}\,\rho(r)\right) r^3\, dr \,. \qquad (28)$$

Here g is the momentum transfer and j_0 and j_1 are spherical Bessel functions. Using the fact that

$$x^2 j_0(x) = \frac{d}{dx}(x^2 j_1(x))$$

and performing a partial integration on $A(\theta)$, one can show that

$$A(\theta) = -\frac{1}{g}\int j_1(gr)(u + iw)\left[\frac{1}{r}\frac{d}{dr}\rho(r)\right] r^3\, dr. \tag{29}$$

Except for the factor $\sin\theta$, $A(\theta)$ and $B(\theta)$ have the same angular dependence and the scattered amplitude can be written as

$$\left(\frac{2m}{\hbar^2}\right)^{-1} f(\theta) = \left(1 + \vec{\sigma}\cdot\vec{n}\sin\theta\ \frac{k^2\mu a^2}{u + iw}\right) A(\theta)\ . \tag{30}$$

The polarization is given then by

$$P = \frac{+\,2k^2 a^2 \mu w/(u^2 + w^2)}{1 + k^4 a^4 \mu^2 \sin^2\theta/(u^2 + w^2)}\ \sin\theta. \tag{31}$$

The polarization is thus independent of the shape of the nuclear potential except that u, w, and μa^2 must be adjusted to yield the experimental total and absorption cross section for a particular choice of the radial dependence. This also predicts that the observed polarization will be the same for all nuclei.[14] Since the result depends on the Born approximation though, this can only be expected to hold for the lightest nuclei.

A similar calculation can be done in the Born approximation using the potentials as defined by Eq. (17). We let

$$a(g) = -a_r(g) - ia_I(g) \tag{32}$$

where a_r and a_I are positive numbers for small values of g (or θ). The differential angular distribution and the polarization are given then by

$$(\hbar^2/2m)\, f(\theta) = \left(a_r + ia_I - i\vec{\sigma}\cdot\vec{n} \sin\theta\, k^2 b\right)(-1/g) \int j_1(gr)\left(\frac{1}{r}\frac{d}{dr}\rho(r)\right) r^3\, dr \,, \tag{33}$$

$$P = \frac{-2k^2 a_I b/|a|^2}{1 + k^2 a_I^2 \sin^2\theta/|a|^2} \sin\theta \,.$$

This is an identical result to Eq. (31) except that the constants u, w, and μa^2 have been replaced by angular dependent functions which will have the effect of modifying Eq. (31) at large angles.

The polarization obtained with the Born approximation can be expected to hold only for forward scattering angles. For larger angles, the angular dependence of $B(\theta)$ relative to $A(\theta)$ changes sufficiently to introduce large corrections to the Born approximation result for the polarization, particularly in the region of the diffraction minima. Thus, it is principally in these latter regions that model dependent features of the polarization can be expected to appear. The more accurate calculations of the next section will bring this out.

B. W.K.B. Approximation

In this section, the scattering problem will be solved in terms of the conventional phase shift expansion. Since it is not possible in general to obtain closed expressions for the phase shifts, it is necessary to appeal to approximate methods. The simplest and most appropriate for this case is the W.K.B. method.

The spin dependent potential of Eq. (23) becomes, when reduced to radial form referring to the ℓ-th partial wave,

$$V_\ell^+ = -(u + iw)\ \rho(r) + \frac{\mu a^2}{r}\ \frac{d}{dr}\ \rho(r)\ \ell$$

$$V_\ell^- = -(u + iw)\ \rho(r) - \frac{\mu a^2}{r}\ \frac{d}{dr}\ \rho(r)(\ell + 1)\ . \tag{34}$$

The superscripts $(+)$ and $(-)$ refer to the spin up ($j = \ell + \frac{1}{2}$) scattered nucleons and spin down ($j = \ell - \frac{1}{2}$) scattered nucleons, respectively.

The ℓ-th phase shifts in terms of the potentials are given in the W.K.B. approximation by the following equation:[15]

$$\delta_\ell^\pm = \int_{}^{\infty} \left[k^2 - \frac{2m}{\hbar^2}\ V_\ell^\pm - \frac{(\ell + \frac{1}{2})^2}{r^2} \right]^{\frac{1}{2}} dr - \int_{}^{\infty} \left[k^2 - \frac{(\ell + \frac{1}{2})^2}{r^2} \right]^{\frac{1}{2}} dr\ , \tag{35}$$

where the lower limits are to be taken at the zeros of the integrands. Under the assumption that $V_\ell^\pm << E$, one obtains by expanding the radical,

$$\delta_\ell^\pm = \frac{1}{2k} \int_y^{\infty} \frac{\left(\frac{-2m}{\hbar^2}\right) V_\ell^\pm(r)\, r\, dr}{\left[r^2 - y^2\right]^{\frac{1}{2}}}\ , \tag{36}$$

$$ky = (\ell + \tfrac{1}{2})\ .$$

It has been pointed out by Fernbach, Serber, and Taylor[16] that this expression is equivalent to their more physical approach to the problem of high energy scattering from a complex potential well.

The expressions $A(\theta)$ and $B(\theta)$ from which the scattering cross section and polarization are to be calculated are given in terms of a phase shift expansion by[5]

$$A(\theta) = \frac{i}{k}\sum_{\ell=0}^{\infty}\left[(\ell+1)\exp(i\delta_\ell^+)\sin\delta_\ell^+ + \ell\exp(i\delta_\ell^-)\sin\delta_\ell^-\right]P_\ell^0$$

$$B(\theta) = -\frac{i}{k}\sum_{\ell=1}^{\infty}\left[\exp(i\delta_\ell^+)\sin\delta_\ell^- - \exp(i\delta_\ell^-)\sin\delta_\ell^-\right]P_\ell^1$$

The various potential models which will be considered and the expressions for the phase shifts obtained from Eq. (36) are as follows:

1. Square well:

$$V_\ell^{\pm} = -(u + iw) - \frac{\mu a^2}{R}\,\delta(r - R)\begin{Bmatrix}\ell\\ -(\ell+1)\end{Bmatrix}, \qquad r \le R$$

$$\delta_\ell^{\pm} = \tfrac{1}{2}\frac{u + iw}{E}(kR)S_\ell + \frac{\mu}{2E}\frac{(ka)^2}{kR}S_\ell^{-1}\begin{Bmatrix}\ell\\ -(\ell+1)\end{Bmatrix}, \qquad \ell \le kR - \tfrac{1}{2}$$

$$\delta_\ell^{\pm} = 0 \qquad \ell \ge kR - \tfrac{1}{2}$$

$$E = \hbar^2k^2/2m, \qquad S_\ell = \left(1 - \left(\frac{\ell+\frac{1}{2}}{kR}\right)^2\right)^{\frac{1}{2}}$$

2. Parabolic well:

$$V_\ell^\pm = -(u + iw)(1 - r^2/R^2) - \frac{2\mu a^2}{R^2} \begin{Bmatrix} \ell \\ -(\ell+1) \end{Bmatrix}, \quad r \leq R$$

$$\delta_\ell^\pm = \tfrac{1}{2} \frac{u + iw}{E} \frac{2}{3} (kR) S_\ell^3 + \frac{\mu}{E} \frac{(ka)^2}{kR} S_\ell \begin{Bmatrix} \ell \\ -(\ell+1) \end{Bmatrix} \quad \ell \leq kR - \tfrac{1}{2}$$

$$\delta_\ell^\pm = 0, \qquad \ell \geq kR - \tfrac{1}{2}$$

$$E = \hbar^2 k^2/2m, \qquad S_\ell = \left(1 - \left(\frac{\ell + \frac{1}{2}}{kR}\right)^2\right)^{\frac{1}{2}}$$

3. Gaussian well:

$$V_\ell^\pm = -(u + iw)\, e^{-\gamma^2 r^2} - 2\mu a^2 \gamma^2 e^{-\gamma^2 r^2} \begin{Bmatrix} \ell \\ -(\ell+1) \end{Bmatrix}$$

$$\delta_\ell^\pm = \tfrac{1}{2} \frac{u + iw}{E} \left(\frac{k\sqrt{\pi}}{2\gamma}\right) e^{-S_\ell^2} + \frac{\mu}{E} a^2 \gamma^2 \left(\frac{k\sqrt{\pi}}{2\gamma}\right) e^{-S_\ell^2} \begin{Bmatrix} \ell \\ -(\ell+1) \end{Bmatrix}$$

$$E = \hbar^2 k^2/2m, \qquad S_\ell = \frac{\gamma}{k} (\ell + \tfrac{1}{2}) \qquad \ell \leq 2/\gamma$$

4. Coulomb potential:

$$V = \frac{Ze^2}{r}, \qquad r > R; \qquad V = \frac{Ze^2}{R}, \qquad r < R$$

$$\delta_\ell^c = \Delta_\ell + \eta_\ell$$

$$\Delta_\ell = \left(\frac{zZe^2M}{\hbar^2k}\right)\left\{\ln\left[\frac{kR(1+S_\ell)}{\ell+\frac{1}{2}}\right] - S_\ell\right\}$$

$$\eta_\ell = \left(\frac{zZe^2M}{\hbar^2k}\right)\ln\left(\ell+\tfrac{1}{2}\right) \qquad \text{[Coulomb phase shift]}$$

$$S_\ell = \left(1 - \left(\frac{\ell+\frac{1}{2}}{kR}\right)^2\right)^{\frac{1}{2}}$$

	Square well	Parabolic well	Gaussian well A	Gaussian well B	Coulomb potential
u(Mev)	0	18	0	53	
w(Mev)	18	30	89	76	
μa^2(Mev-cm^2)	5×10^{-26}	4.77×10^{-26}	9.85×10^{-26}	17.6×10^{26}	
R(cm)	$1.4A^{\frac{1}{3}}10^{-13}$	$1.6A^{\frac{1}{3}}10^{-13}$			$1.25A^{\frac{1}{3}}10^{-13}$
$\frac{1}{\gamma}$ (cm)			$(\frac{2}{3})^{\frac{1}{2}}A^{\frac{1}{3}}10^{-13}$	$(\frac{2}{3})^{\frac{1}{2}}A^{\frac{1}{3}}10^{-13}$	

TABLE I

Numerical Values of the Nuclear Well Parameters Used in the Calculations.

The values of u, w, μa^2, and the radius or shape parameter must now be picked for each well shape, so that the calculated total and differential scattering cross sections for a given well shape agree with the experimental cross sections. Unfortunately, the measured neutron-nucleus cross sections at 300 Mev are not sufficiently extensive or precise to fix the potentials unequivocally. The values of u, w, μa^2, and R which are used are consistent with the available data[17] and serve as representative values. These are given in Table 1. The central potential for the square well is given by Fernbach.[16] The central potentials and radii for the parabolic and gaussian wells have been determined by a similar analysis for these well shapes.[18] The values of the spin-orbit potentials which are given correspond roughly to the same volume as a square well of radius 3×10^{-13} cm and a depth of about 1 Mev. This is also about the same strength as the spin-orbit potential of the shell model.[19] Unless the actual value departs greatly from this, this should serve as a representative value.

To calculate the coulomb phase shifts it was assumed that the coulomb potential was constant for distances less than the indicated radius, regardless of the assumed nuclear well shape. This was done for numerical simplicity and should yield representative results.

The scattering cross section and polarization has been evaluated by the above method and for the above potentials for 290 Mev neutrons incident in carbon. These results are given in Figs. 1 to 4. The scattering cross section and polarization has also been evaluated for 290 Mev neutrons and protons incident on aluminum[20] for a parabolic well shape. These results are given in Figs. 5 and 6.

In addition to the above calculations, the scattering cross section and polarization was also evaluated for 290 Mev neutrons on carbon for the case where both central and spin-orbit potentials were square wells. The potential taken was

$$V_\ell^{\pm} = \left[-(0 + i\,18) - 2 \begin{Bmatrix} \ell \\ -(\ell+1) \end{Bmatrix} \right] \text{Mev}, \qquad r \leq R.$$

This calculation, besides being done by the W.K.B. method, was also done by an exact phase shift calculation[21] on the UNIVAC at the University of California Radiation Laboratory at Livermore. The results for the polarization are given in Fig. 7. The angle at which the peak value of the polarization occurs is shifted to the left by a few degrees by the approximate method. Otherwise the two results are in essential agreements thus giving some idea of the validity of the W.K.B. approximation in these calculations.

On the basis of these numerical results, a number of qualitative features of the scattering process, which reflect a dependence on the nuclear well shape and associated parameters, become immediately apparent. Aside from their bearing on the interpretation of the experimental results they are of some interest of themselves.

(a) Differential angular cross section:

A comparison of the calculated differential cross sections for the square well, parabolic well, and gaussian well shapes, shows the effect on the angular distribution by the rounding off of the potential distribution. The rounding of the well shape decreases the magnitude of the second maximum relative to the first and moves it to larger angles. The effect is most pronounced in the gaussian. It is of interest to note that the minima and secondary maxima still persist in the gaussian, since in the Born approximation

treatment of a gaussian potential shape, these effects are absent.

In addition one notes that the troughs of the first defraction minima are relatively shallow as compared with the usual calculations. This reflects the presence of the scattering caused by the spin orbit potential, which tends to fill up the trough of the minima. This is of interest since these deep minima have never been observed experimentally in the scattering of nucleons from nuclei.

(b) Polarization:

The calculated results show that in all the cases considered large polarizations are obtained. The magnitude of the polarization does not reflect to any extent model dependent features for parameters of the general values chosen. One notes from an examination of the Born approximation result that the polarization will be small only if the real central potential is large compared to the imaginary central potential. This situation does exist for nucleon energies below 100 Mev and one would therefore expect the measured polarization to be considerably smaller at lower energies.[22]

The sign of the polarization is negative (excluding the small region of the dip). This means physically that an incident beam which is polarized perpendicular and "upward" to the incident direction and plane of scattering will be preferentially scattered to the left (Eq. 27). If the sign of the spin orbit potential is reversed, the sign of the polarization will be reversed. The change in magnitude and shape of the polarization curve will be neglibible.

The most striking feature of the results is the double reversal in the sign of the polarization in the neighborhood of the first diffraction minimum. This double reversal of sign or dip is a consequence of the fact

that the functions $A(\theta)$ and $B(\theta)$ in the scattered amplitude have slightly different periods of oscillation. The dip may be regarded as a diffraction phenomenon. A comparison of the results for the various potential shapes show that if the real potential is zero (or sufficiently small) compared to the imaginary potential, the dip is not eliminated by the rounding off of the square well. If, however, the real potential is increased sufficiently relative to the imaginary central potential, the dip is essentially eliminated. Furthermore, for a given central potential, the dip is made more prominent as the radius is increased, as illustrated by the calculations for carbon and aluminum using the parabolic well. It should be noted that the inclusion of the coulomb potential so as to describe the scattering of protons, decreases the magnitude of the first maximum of the polarization and widens the angular width of the dip. Thus, the dip is more easily resolved with protons than with neutrons, aside from experimental considerations.

IV. COMPARISON WITH EXPERIMENT

The measured differential cross sections and polarizations obtained by Chamberlain, Segre, Tripp, Wiegand, and Ypsilantis[23] for the scattering of 290 Mev protons from α-particles, carbon, and aluminum are shown in Figs. 8, 9, and 10. These results are also included (without noting the experimental errors) in the previous figures one through six. The experimental angular cross sections which are drawn as a dashed lines in Figs. 1, 2, and 5 are the arithmetic average of the left and right scattering; that is, the differential angular cross section for an unpolarized incident beam.

One notes first the similarity between the polarization for α-particles and carbon targets that exists out to an angle of about 30°. This experimental result is in qualitative agreement with the Born approximation result that the polarization is independent of the target nucleus.

Aside from this qualitative agreement with the theory, a detailed comparison of the experimental results with the calculated results show rather significant discrepancies, particularly for carbon. One notes, for carbon, that there is neither a first diffraction minimum or a dip in the polarization. The second maximum for the square and parabolic wells is larger than the experimental cross section at the same angle; while for the gaussian well the calculated cross section falls below the experimental cross section at the larger angles. The question of the presence or absence of a dip in the measured polarization for carbon can be put aside because of uncertainties in the nuclear well shape and associated parameters. The principal discrepancy with respect to the polarization is at large angles where one finds that the experimental polarization drops off to essentially zero,

while the calculated polarizations remain large except in the immediate neighborhood of the dip. The latter situation also exists for aluminum, where, although the dip in the polarization exists in qualitative agreement with the calculated results, there is a discrepancy at the larger angles similar to that for carbon.

One can look for the origin of these discrepancies in two possible directions. First, there are the experimental difficulties associated with the large angle scattering. Secondly, there is the question of the validity of the assumed potentials for describing the scattering at the large angles. These two points will be considered in order.

Aside from the experimental difficulties imposed by the low intensities and the requirements of angular definition, that have been met in the data presented, the principal difficulty exists in the separation of the purely elastic scattering from the inelastic scattering corresponding to the excitation of the low lying nuclear levels. The data as presented certainly includes some amount of this inelastic scattering. In the forward directions where the elastic scattering cross section is large the inelastic scattering undoubtedly offers no problem. At large angles (say $\gtrsim 20^{\circ}$) the two could easily be comparable.[23] It is known that for the scattering of 100 Mev nucleons from carbon[24] the differential cross section for exciting the low lying nuclear levels is comparable to the elastic scattering cross section at large angles. If this is the case at 300 Mev, the inclusion of this inelastic scattering with the elastic might result in the filling up of the diffraction minima.[25] The presence of the inelastic scattering would tend to resolve the difference between the calculated and experimental cross sections

for the larger angles if one assumes a gaussian well shape. It is not apparent that this would be so for the assumption of square or parabolic wells. In addition, since the inelastically scattered particles would not be expected to be polarized as much as the elastically scattered particles, the inclusion of some inelastic scattering would "dilute" the polarization of the elastic scattering and possibly account for the smallness of the measured polarization.

An observation which seems to contradict at least the latter statement, is the striking similarity between the polarization obtained for helium and carbon targets. For certain, the inelastic scattering from the α-particle is of a negligible amount; which (assuming the Born approximation result) leads one to believe that the inelastic scattering present in the carbon data does not change the polarization appreciably.

The preceding discussion suggests that some of the discrepancy between the experimental and calculated results can be attributed to the effect of an inadequate representation of the nucleon-nucleus interaction. The discussion in Section II pointed out that an arbitrary potential well model will not be likely to describe the large angle scattering accurately, since it must contain implicitly a description of the nucleon-nucleon scattering. To the extent that the Born approximation is valid, this is seen directly in Eq. (33). It is apparent that the angular behavior of the functions $a(g)$ and $b(g)$ will modify both the angular distribution and the polarization which is obtained from a simple well model. The polarization in particular will show this modification, since for the lightest nuclei the angular dependence of the polarization is characterized entirely (except for the factor $\sin\theta$) by the functions $a(g)$ and $b(g)$. These functions are probably decreasing functions

of the angle in the angular range of interest here. The discrepancy between the calculated and measured polarizations can probably be ascribed to this circumstance.[26] Conversely, for a light target such as the α-particle, the measured polarization offers a further condition on the nucleon-nucleon interaction beyond that which can be obtained from nucleon-nucleon scattering experiments.

The lack of a diffraction minimum and secondary maximum for carbon and their rather minor character for aluminum is probably more a reflection of the well shape than the angular behavior of the functions $a(g)$ and $b(g)$. From these calculations no definite conclusions on the well shape can be drawn, though they certainly suggest the necessity of a long tailed potential well. The uncertainty introduced by inelastic scattering is, of course, not to be ignored.

The calculated polarization for aluminum is in qualitative agreement with the experimental result. The discrepancy at the larger angles can be ascribed to the same basic reason as before. Since, however, the Born approximation has ceased to be valid for this case, the angular dependence of the polarization is no longer characterized by $a(g)$ and $b(g)$ alone. It should be noted that for the particular parameter associated with the parabolic well, the dip in the polarization is effectively suppressed for carbon, but does occur for aluminum. The fact that the dip in the calculated polarization occurs at a somewhat smaller angle than is experimentally observed may be a result of the approximate nature of the calculation (see Fig. (7)).

The calculated differential angular cross section of protons scattered from aluminum is larger than the experimental cross section in the angular

region 8° to 15°. This indicates that the real central potential used is too large and should be reduced (changes in the real potential have a small effect on the total cross section at these energies). This would also increase the polarization in the same angular range as above and increase the width of the dip. This would improve the agreement between the calculated and measured polarization.

It should be noted that the coulomb potential has a substantial effect on the polarization of protons scattered from aluminum (and naturally for heavier target nuclei also) for angles less than $\sim 15^{\circ}$. The interference between the nuclear scattering and the coulomb scattering offers in principle a method of determining the sign of the polarization. However, neither the calculations nor the experimental results are sufficiently precise as they stand to establish the sign of the polarization.

In connection with the preceding observations, the results of the calculations of Tamor[27] for the polarization of nucleons scattered from spin zero nuclei should be noted. His calculation is done in the impulse approximation and thus his result is equivalent to that of Eq. (33). He has in addition, however, expressed the transition matrix in terms of the nucleon-nucleon phase shifts and used the numerical values for the phase shifts given by Goldfarb and Feldman, and Swanson.[28] The spin dependence of the nucleon-nucleon potential is given by a tensor force. Tamor's results are in qualitative agreement with the experimental results and our calculations. One point of particular interest is the sign of the polarization which he obtains, which is negative. This agrees with the sign which we have obtained

using a spin-orbit potential of the same sign as the shell model spin-orbit potential. Accordingly, the tensor force leads to the same sign of the spin-orbit potential at these energies as that of the shell model.[29] A comparison of his numerical results with Eq. (31) also leads to an estimate of the magnitude of the spin-orbit potential. This can be simply done and yields a value of the order of one Mev ($\mu \sim 1$ for $a = 3.10^{-13}$ cm; Eq. (22)).

SUMMARY

The spin dependence of the nucleon-nuclear interaction must be of a spin-orbit form and it was shown that the radial form of the spin-orbit potential is to a first approximation proportional to $\frac{1}{r}\frac{d}{dr}$ of the central potential. This result was obtained assuming the impulse approximation and neglecting the role of multiple scattering. In addition, it was pointed out that the optical model potential must implicitly contain the characteristics of the nucleon-nucleon scattering in order to describe large angle nucleon-nucleus scattering.

The differential angular cross section and the polarization of nucleons was calculated in the Born approximation and on the W.K.B. approximation. To the extent of the validity of the Born approximation, the polarization is independent of the size and shape of the nucleus. This result can only be expected to hold for the lightest nuclei and for forward scattering angles. The experimental results for the polarization of protons scattered from helium and carbon are very similar out to angle of 30° and bear this result out. The W.K.B. calculations were made for square, parabolic, and gaussian well shapes. The parameters associated with these well shapes were chosen to fit the measured total and elastic scattering cross sections for 300 Mev neutrons. The strength of the spin-orbit potential was chosen in every case to correspond roughly to a square well of one Mev depth and radius equal to that of carbon. A large degree of polarization was obtained in every case, so that the magnitude of the polarization does not reflect model dependent features. The most striking characteristic of the polarization is the double reversal of the sign of the

polarization in the immediate region of the diffraction minima, and may itself be regarded as a diffraction phenomena. It was found that the presence of the dip in the polarization depends on the relative magnitude of the real to the imaginary central potentials and on the size of the nucleus. A comparison of these calculated cross sections and polarizations with the experimental results for carbon showed in general a rather poor agreement. The calculated polarization remains large at large angles except in the neighborhood of the dips while the measured polarization becomes quite small at an angle of 30°. Although experimental uncertainties introduce some ambiguity in the interpretation, the discrepancy at large angles can undoubtedly be attributed to the inadequacy of the optical model potentials used. For, as pointed out, the large angle scattering depends to some extent on the details of nucleon-nucleon scattering, which must therefore be incorporated into the optical model potential. The experimental and calculated results for aluminum show a somewhat better agreement since a larger part of the elastic scattering is confined to smaller scattering angles.

A comparison of these calculations with those of Tamor's in which he utilized the calculated nucleon-nucleon scattering amplitudes show that the tensor force in the nucleon-nucleon interaction leads to a spin orbit potential at these energies of the same sign as the spin-orbit potential of the shell model. A further comparison shows also that the magnitude of the spin-orbit potential used in these calculations is consistent with the nucleon-nucleon tensor interaction.

We wish to thank Drs. O. Chamberlain, E. Segre, C. Wiegand, and Messrs. R. Tripp and T. Ypsilantis for the many discussions relating to their experimental measurements. We wish to thank Dr. Stephen Tamor and Dr. Malvin Ruderman for conversations relating to the polarization phenomena. It is a pleasure to express our appreciation to Mrs. Mary Harrison and Miss Harriet Cox for their excellent computational work. This work was performed under the auspices of the Atomic Energy Commission.

REFERENCES

1. N. C. Francis and K. M. Watson, Phys. Rev. 92, 291 (1953).

2. E. Fermi, Nuova cimento 11, 407 (1954); W. Heckrotte and J. V. Lepore, Phys. Rev. 94, 500 (1954); B. J. Malenka, Bull. Am. Phys. Soc. 29, No. 4, 32 (1954); G. A. Snow, R. H. Sternheimer, and C. N. Yang, Phys. Rev. 94, 1073 (1954); R. H. Sternheimer, Phys. Rev. 95, 587 (1954).

3. S. Fernbach, R. Serber, and T. Taylor, Phys. Rev. 75, 1352 (1949).

4. R. Serber, Phys. Rev. 72, 1114 (1947).

5. J. V. Lepore, Phys. Rev. 79, 137 (1950).

6. W. F. Ball, University of California Radiation Laboratory Report-1938.

7. For non-spin zero nuclei, one would expect terms in the nucleon-nucleus potential like $\vec{\sigma}\cdot\vec{I}$ and $\vec{L}\cdot\vec{I}$ where $\vec{I}$ is the nuclear spin. These terms would not be expected to be as significant as the $\vec{\sigma}\cdot L$ term.

8. W. Heisenberg, Theorie Des Atomkernes (Gottingen, 1951), p. 22.

9. L. Wolfenstein, and J. Ashkin, Phys. Rev. 85, 947 (1952); R. H. Dalitz, Proc. Phys. Soc. A, Vol. LXV, p. 175 (1952).

10. G. F. Chew, Phys. Rev. 80, 196 (1950).

11. G. F. Chew and G. C. Wick, Phys. Rev. 85, 636 (1954); N. Francis and K. Watson, loc. cit.

12. R. Jastrow, Phys. Rev. 82, 261 (1951); M. Lax, Revs. Modern Phys. 23, 287 (1951); N. Francis and K. Watson, loc. cit.

13. E. Fermi, loc. cit.

14. S. Tamor, Phys. Rev. 94, 1087 (1954); W. Heckrotte, Phys. Rev. 94, 1797 (1954).

15. R. Langer, Phys. Rev. 51, 669 (1937); N. F. Mott and H. S. W. Massey, Theory of Atomic Collisions, 2nd ed. (Oxford, 1949), p. 127.

16. S. Fernbach, R. Serber, and T. Taylor, loc. cit.; S. Fernbach, thesis, University of California Radiation Laboratory Report-1382.

17. W. F. Ball, loc. cit.; J. DeJuren and B. J. Moyer, Phys. Rev. 81, 919 (1951).

18. W. Heckrotte, Phys. Rev. 95, 1279 (1954).

19. J. H. D. Jensen and M. G. Mayer, Phys. Rev. 85, 1040 (1952).

20. We ignore the fact that aluminum has a spin.

21. This choice of spin-orbit potential was dictated by the circumstances that the machine had only been coded for square-well potentials.

22. H. Bradner and R. Donaldson (private communication) have found that the polarization drops in magnitude sharply below incident energies of 135 Mev. This corresponds to the energy region in which the real potential is increasing with decreasing incident energy (see R. Jastrow, reference 11).

23. O. Chamberlain, E. Segre, C. Wiegand, R. Tripp, and T. Ypsilantis, Phys. Rev. 93, 1430 (1954), Phys. Rev. 95, 1105 (1954), and University of California Radiation Laboratory Report-2684 (to be published).

24. K. Strauch and W. F. Titus, Phys. Rev. 95, 854 (1954).

25. We wish to thank Dr. M. Ruderman for conversations relating to this point.

26. The zero in the polarization for the helium target which occurs at $\sim 28^{\circ}$ is certainly to be ascribed to a zero of the function b(g).

27. S. Tamor, Phys. Rev. (to be published).

28. G. J. B. Goldfarb and D. Feldman, Phys. Rev. 88, 1099 (1952); and D. R. Swanson, Phys. Rev. 89, 749 (1953).

29. It has been demonstrated by Feingold (Princeton University thesis, 1950) using a variational calculation that the tensor force leads to the correct splitting (i.e., sign and magnitude) of the $J = 3/2, 1/2$ levels of Li^7. This circumstance together with the above leads one to believe that the sign of the polarization is indeed as predicted by Tamor.

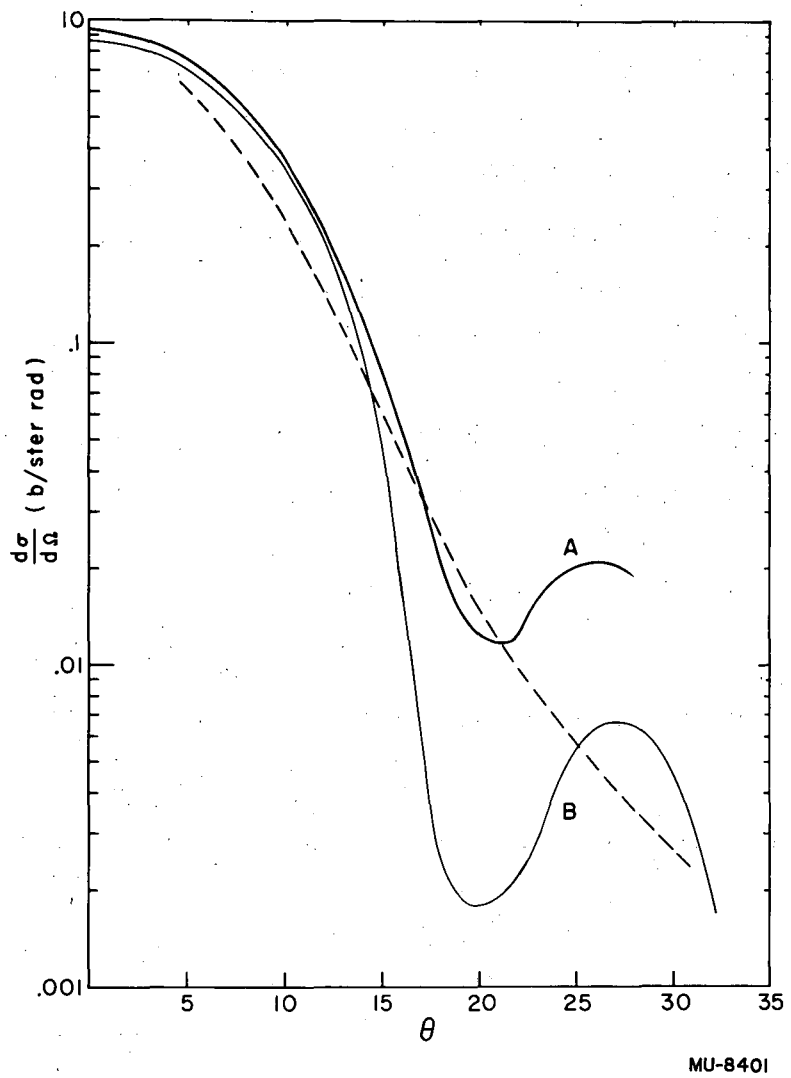

Fig. 1 Differential Angular Cross Section for Unpolarized Incident Neutrons Elastically Scattered from Carbon Assuming (A) a Square Well Central Potential and (B) a Parabolic Well Central Potential. The Dotted Line Gives the Experimental Result.

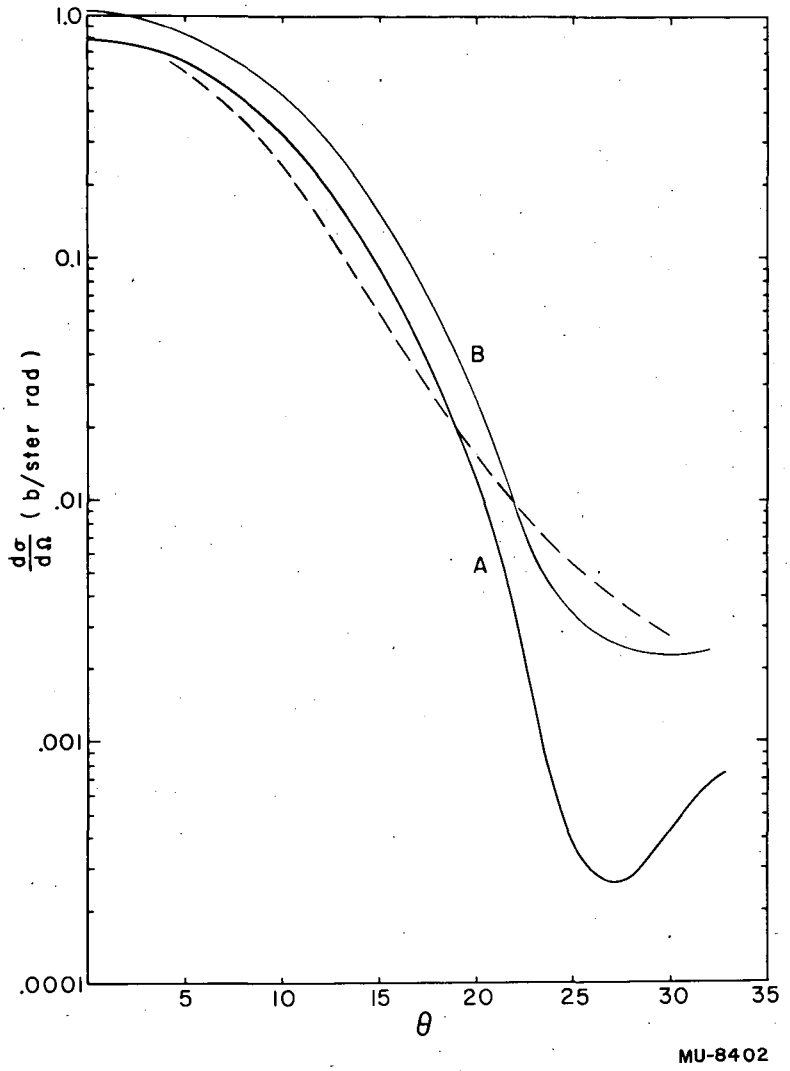

Fig. 2 Differential Angular Cross Sections for Unpolarized Incident Neutrons Scattered from Carbon Assuming a Gaussian Well Central Potential for Two Different Well Depths (see Table 1). The Dotted Line Gives the Experimental Result.

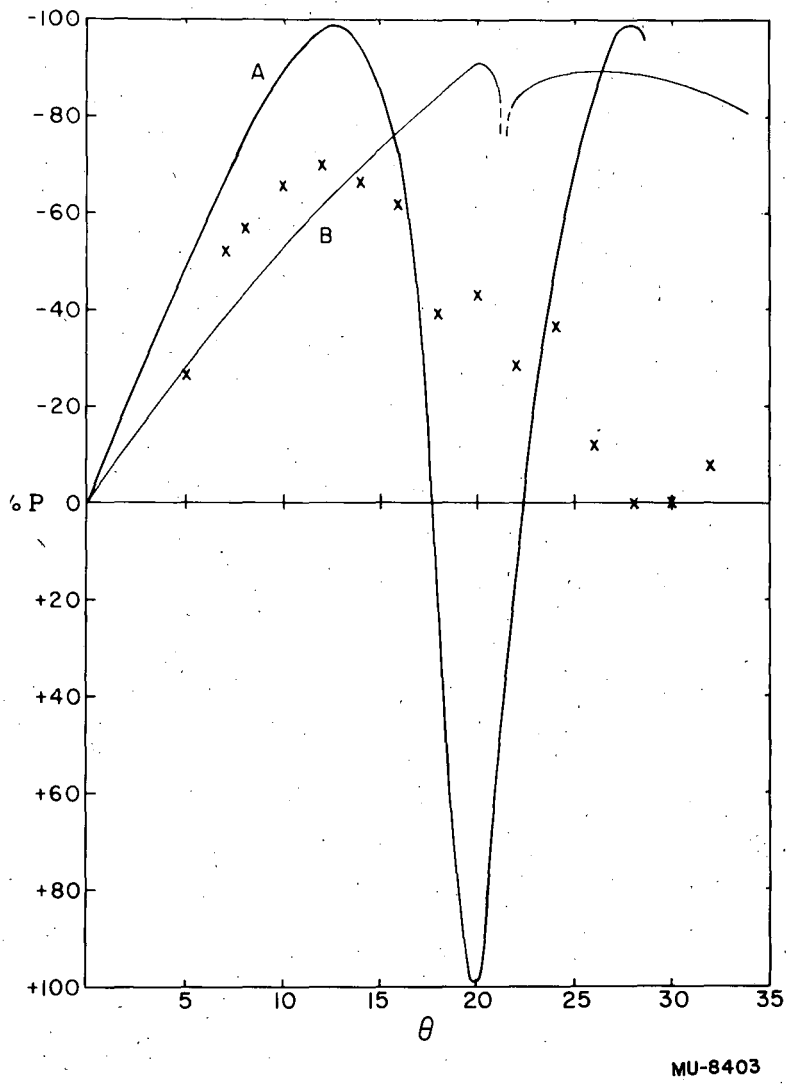

Fig. 3 Polarization of Neutrons Scattered from Carbon Assuming (A) a Square Well Central Potential and (B) a Parabolic Well Central Potential. The Crosses Give the Experimental Results.

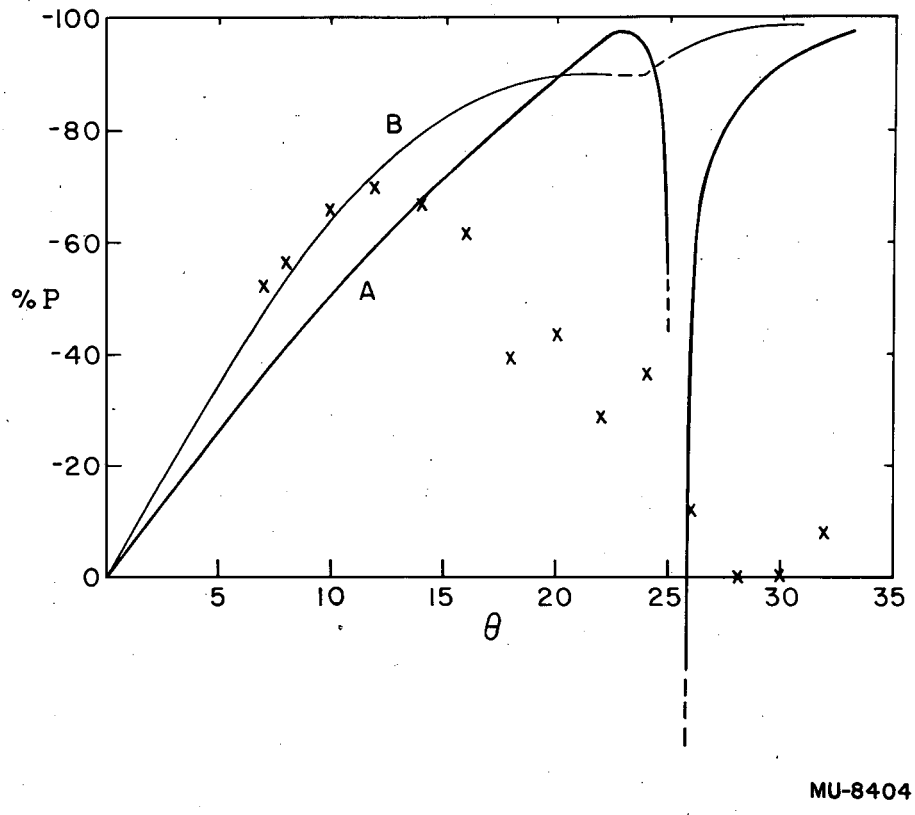

Fig. 4 Polarization of Neutrons Scattered from Carbon Assuming a Gaussian Well Central Potential for Two Different Well Depths (see Table 1). The Crosses Give the Experimental Results.

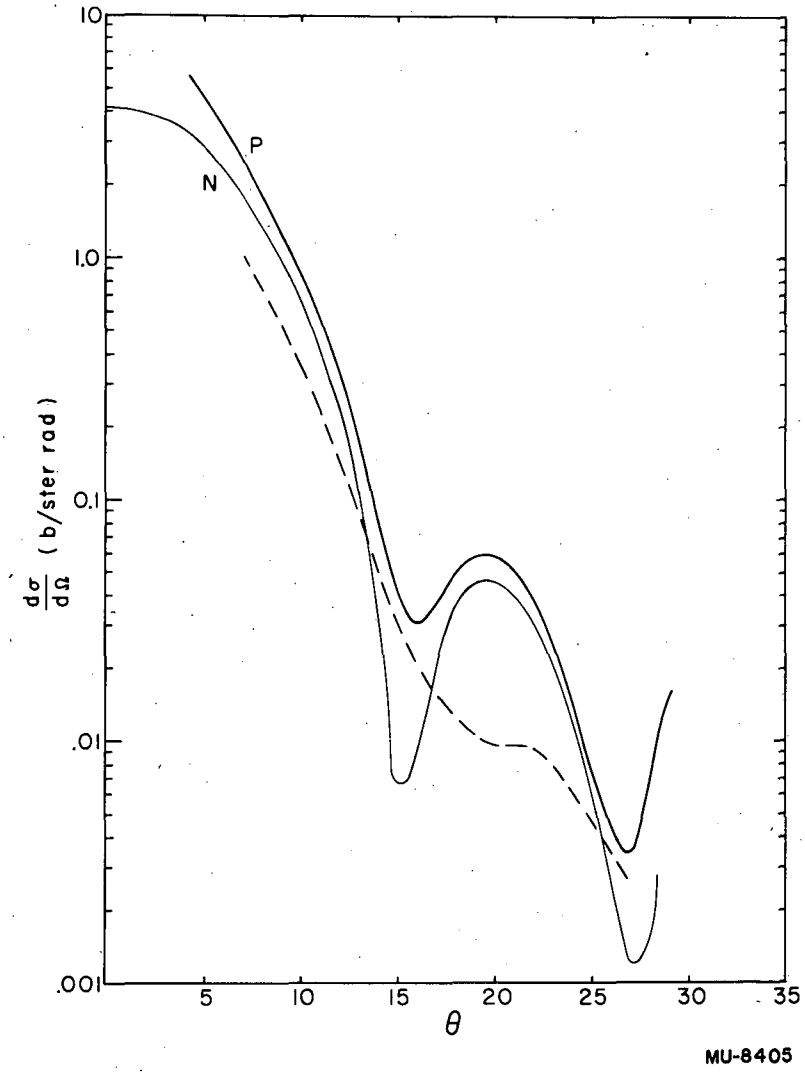

Fig. 5 Differential Angular Distribution for Unpolarized Incident Neutrons (N) and Protons (P) Scattered from Aluminum Assuming a Parabolic Well Central Potential. The Dashed Line Give the Experimental Result.

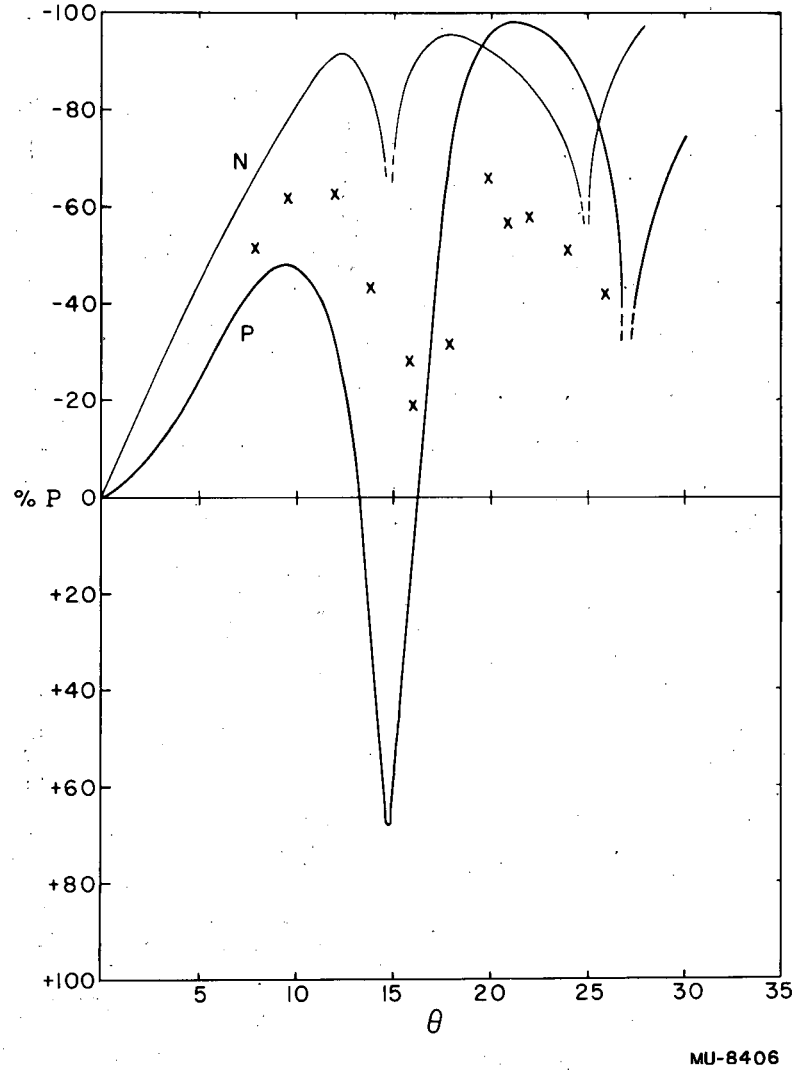

Fig. 6 Polarization of Neutrons (N) and Protons (P) Scattered from Aluminum Assuming a Parabolic Central Potential. The Crosses Give the Experimental Results.

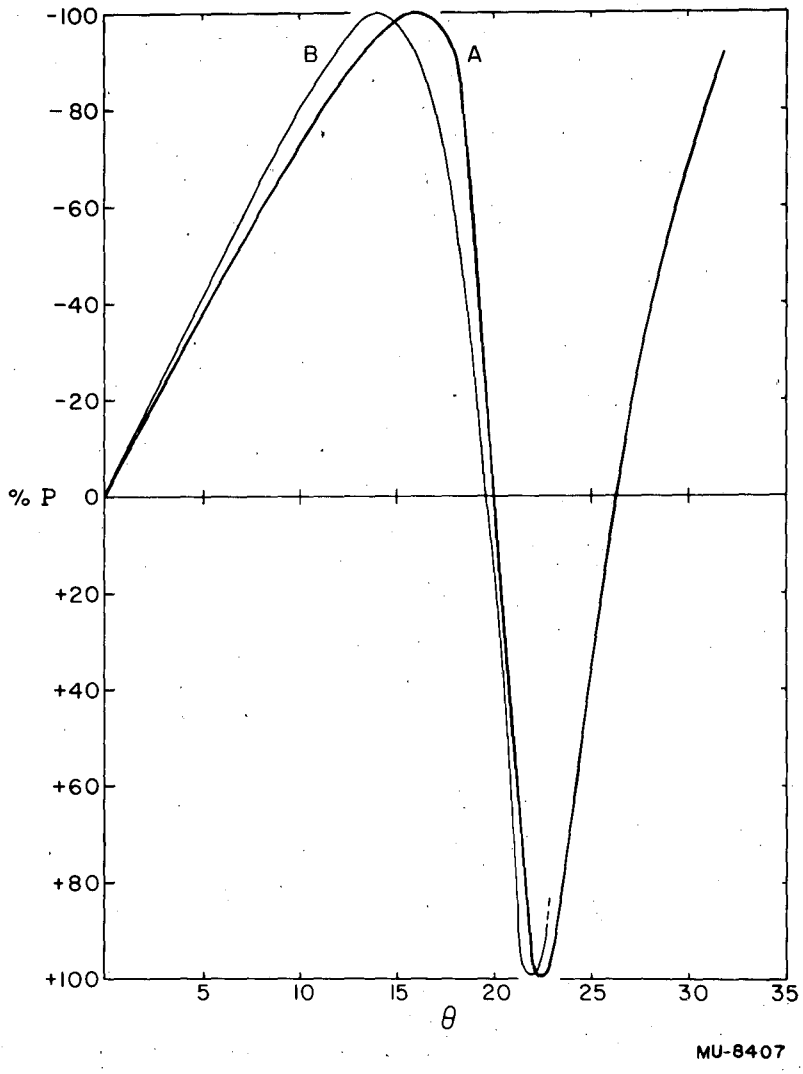

Fig. 7 Polarization of Neutrons Scattered from Carbon Assuming a Square Well Central and Spin Orbit Potential. Curve A Shows the Result of a Machine Calculation, and Curve B Shows the Result of the Approximate Method Used in the Rest of the Calculations.

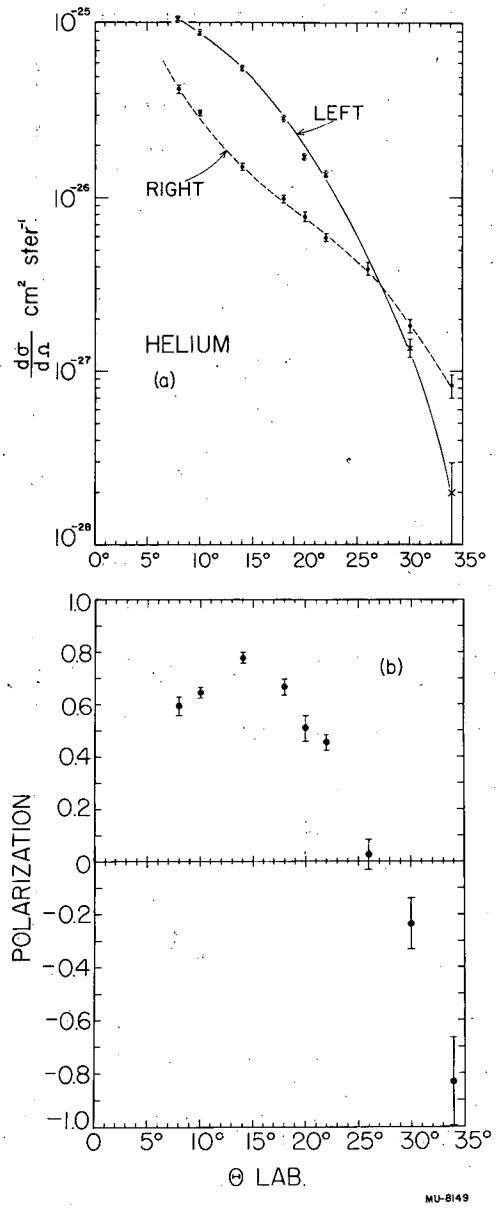

Fig. 8 (a) Differential Scattering Cross Section Versus Left and Right Scattering Angles for 74% Polarized 315-Mev Protons Scattered Elastically by Helium.
(b) Polarization of Protons Scattered by Helium Versus Scattering Angle.

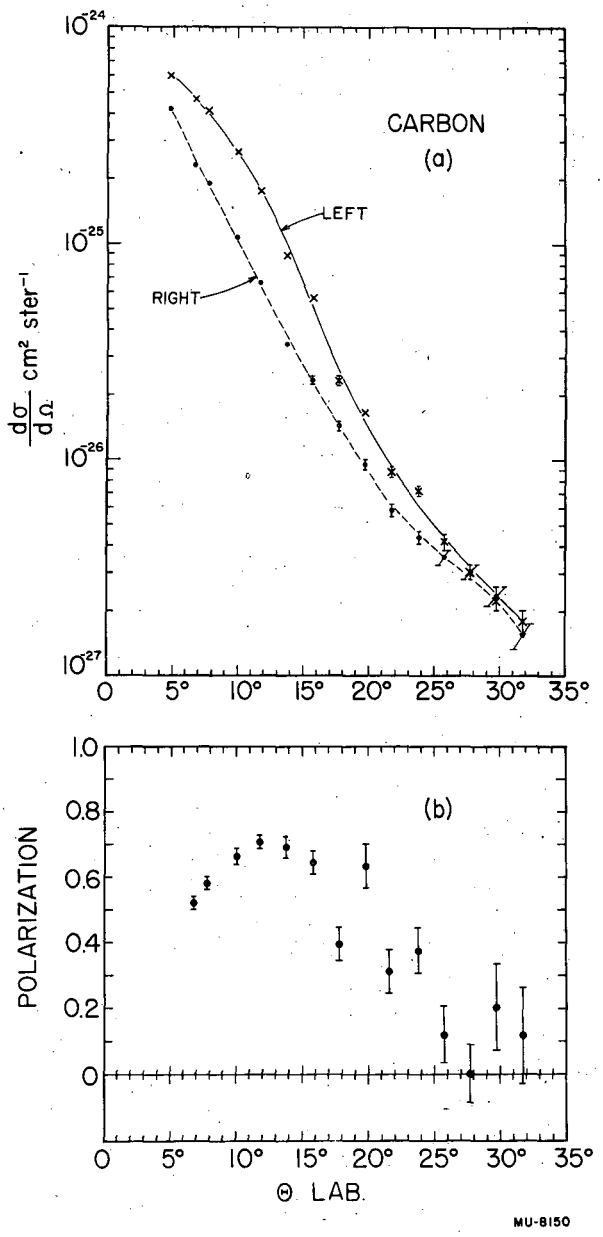

Fig. 9 (a) Differential Scattering Cross Section Versus Left and Right Scattering for 64% Polarized 290-Mev Protons Scattered Elastically by Carbon.
(b) Polarization of Protons Elastically Scattered by Carbon Versus Scattering Angle.

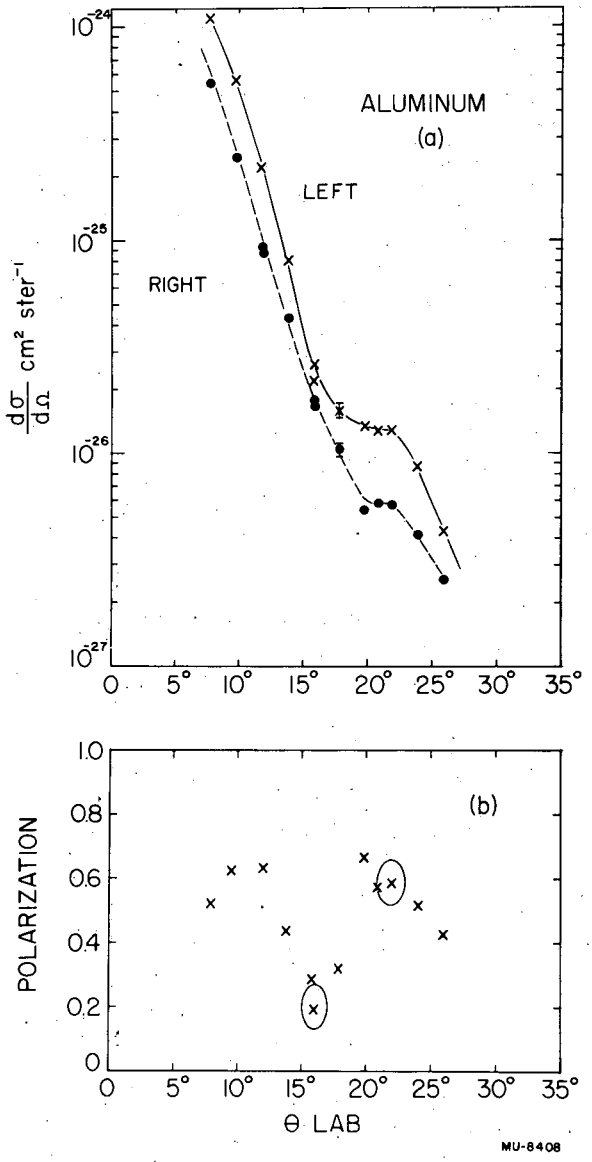

Fig. 10 (a) Differential Scattering Cross Section Versus Left and Right Scattering for 64% Polarized 290-Mev Protons Scattered Elastically by Aluminum. Typical Errors are Indicated.
(b) Polarization of Protons Elastically Scattered by Aluminum Versus Scattering Angle. Typical Errors are Indicated.